Measurement of the Vertical Distribution of Reflected Solar Radiation*

Tetsu Aoki[1] & Akio Mizutani[2]

[1]Dept. of Architecture, National Institute of Technology, Gifu College,
2236-2 Kamimakuwa, Motosu City, Gifu Pref., Japan
[2]Dept. of Architecture, Nagoya Institute of Technology,
Gokiso-cho, Showa-ku, Nagoya, Aichi Pref., 466-8555 Japan
Email: aokilab@gmail.com

Abstract. The purpose of this study was to develop a device for measuring the vertical distribution of the reflected radiation to the inside of a room from terrace to building. The proposed device is attached to aluminum plates that are painted matte black at intervals of 20 cm on polystyrene insulation. The surface temperature of the aluminum plate, called the *SAT* (sol-air temperature), is used as an indicator of the quantity of solar radiation. In order to compare terrace materials, two of the measuring devices were located facing south. Concrete tile, artificial turf, and wood chips were selected as materials to be compared for the surface of the terrace and were laid in front of the measuring devices. The results indicate that the *SAT* reflected onto a vertical plane was higher closer to the ground for all materials. Hourly fluctuations of the vertical distribution of the reflected solar radiation differed, depending on the terrace surface material. When concrete tiles of different thicknesses were compared, the temporal heating patterns varied due to differences in heat capacity. These results lead us to the conclusion that using the developed measuring device enables grasping the effect of vertical distribution of reflected solar radiation from a terrace.

Keywords: *long-wave radiation; measuring device; material of terrace; reflected solar radiation; vertical distribution.*

1 Introduction

There are several methods for reducing the cooling load of a building by reducing the solar radiation heat entering into its interior. The outside of buildings can be covered with solar radiation shelters like trees and wall greenery to keep the walls from being directly exposed to solar radiation [1,2]. Color with high solar reflectance can be applied to roofs and external walls to control their surface temperature [3,4]. Glass that is made highly reflective by low-emissivity coating is used in windowpanes to control the solar radiation passing into the interior [5].

Received April 2nd, 2014, Revised July 26th, 2014, Accepted for publication January 27th, 2015.
 ISSN: 2337-5779, DOI: 10.5614/j.eng.technol.sci.2015.47.2.5
*Part of this paper has been presented in The 2nd International Conference on Sustainable Infrastructure & Built Environment (SIBE), 19-20 November 2013, Bandung, Indonesia.

For reducing cooling loads it is important to consider the influence of reflected solar radiation from the ground surface in addition to that of direct rays. In particular, thermal effects from both direct rays and reflected solar radiation are high for window glass [6]. Moreover, understanding the vertical distribution of reflected solar radiation could help in designing thermal barriers. For this reason, a method of calculating direct and reflected solar radiation for vertical surfaces was suggested in [7]. But the physical properties of surface materials need to be taken into consideration. Figure 1 shows the concept of vertical distribution of solar radiation into a room. If it is possible to measure the vertical distribution of reflected solar radiation, this will be helpful in planning the terrace material and the height of the room's windows.

In order to take heat from solar radiation into consideration, in architectural environmental engineering the *solar heat gain coefficient* [8] is used for windowpanes and the *SAT* (*sol-air temperature*) [9] for walls. The *SAT* is represented by the sum of the outdoor temperature and the rise in virtual outdoor temperature that would be required to replace the solar radiation heat that enters through the surface of the building.

The purpose of this study is to develop a device for measuring the vertical distribution of the reflected radiation from a terrace that utilizes the principle of *SAT*.

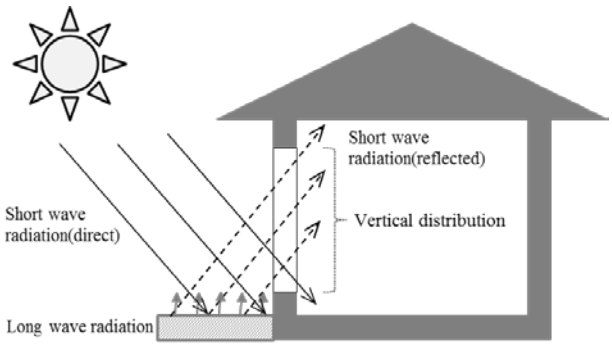

Figure 1 Concept of vertical distribution of solar radiation.

2 Experiment

SAT is applicable only with thin materials for which the material's calorific capacity can be disregarded [9]. Thus, thin aluminum was selected as the material for the *SAT* meter. Since the aluminum plate is flat, unlike the radiometer, it is easy to grasp the effect of radiation and it doesn't make a shadow on the vertical surface. Also, the measurement device is not complicated when it is only used for measuring the surface temperature of the aluminum plate. The developed *SAT* meter is based on the following measurement principles.

Aluminum plates are attached to the front side of a sheet of thermal insulation and are painted with a matte black paint with a solar absorptivity and emissivity of about 1 (Figure 2). The heat budget for the device is shown in Eq. (1). When short- and long-wave solar radiation hit the *SAT* meter, they are changed into heat on the aluminum surface.

$$q = \mathrm{a}I_s - \varepsilon I_L - \alpha (T_s - T_o) \tag{1}$$

Eq. (1) can be rearranged into Eq. (2).

$$\begin{aligned} q &= \alpha \left[\left(T_o + \frac{\mathrm{a}}{\alpha} I_s - \frac{\varepsilon I_L}{\alpha} \right) - T_s \right] \\ &= \alpha (SAT - T_s) \end{aligned} \tag{2}$$

Since the backside of the *SAT* meter is insulated, the heat is not conducted and all the heat from the surface of the aluminum is dissipated by convection and radiation transfer. Thus *SAT* and T_s are nearly equal and *SAT* can be expressed as shown in Eq. (3).

$$SAT = \frac{1}{\alpha}(\mathrm{a}I_s - \varepsilon I_L) + T_o \tag{3}$$

The measuring device was made by attaching aluminum plates, 11 cm long by 5 cm wide and painted matte black, at intervals of 20 cm to a 2.4 m high sheet of polystyrene insulation (Figure 3). The surface temperature of the *SAT* meter was measured using a copper-constantan thermocouple.

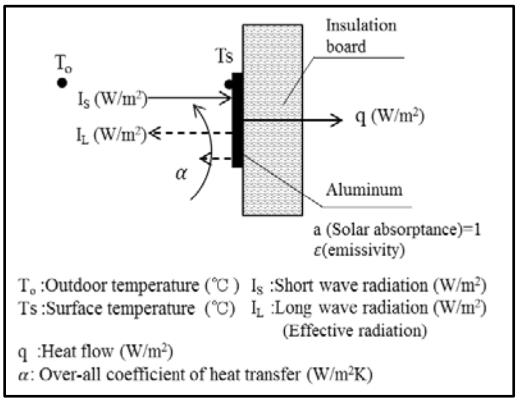

Figure 2 *SAT* meter heat budget.

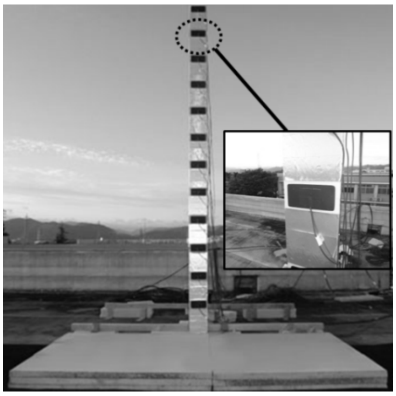

Figure 3 Measuring device and *SAT* meter.

The reason for leaving a space between the aluminum plates is to prevent heat transfer by thermal conduction and to not to make a shadow of the thermocouple on the plate.

In order to compare terrace materials, two of the measuring devices were located facing south on the roof of a three-story RC building on the campus of National Institute of Technology, Gifu College. There were no trees or buildings that blocked the sun from the building roof.

Concrete tile, artificial turf, and wood chips were selected as materials and were laid out in a space–1.8 m long by 0.9 m wide–in front of the measuring devices. The size of the material-covered area was based on a typical general terrace or veranda in Japanese buildings. To prevent reflection from the roof surface from reaching the devices, the roof in front of them was covered by butter muslin. On one side of the two devices (called device A and B), solar radiation and the amount of radiation reflected from the test material were measured using a four-component radiometer at 10-minute intervals. The wind was measured with a two-dimensional anemometer at 1-minute intervals. The measurements were carried out between August and September of 2012.

3 Result and Discussion

3.1 Effect of Concrete Thickness

90-mm thick concrete tiles were placed in front of device A and 30-mm thick concrete tiles were placed on 60 mm of thermal insulation in front of device B. Figure 4 shows the vertical temperature distribution as measured by the *SAT* meter at specific times on August 12. The value is a 30-minute average of every 10 minutes. The dashed line in Figure 4 is the calculated height that would be affected by solar radiation if the material of the terrace diffused the radiation perfectly. The data of solar altitude were obtained from the National Astronomical Observatory of Japan [9].

The *SAT* became higher approaching the surface of concrete during the daytime, indicating that reflected heat influences the temperature. The *SAT* of device B (30-mm concrete) was higher in total than that of device A (90-mm concrete) at 12:00.

Figure 5 shows the surface temperatures (M_s) of the 30-mm and 90-mm concrete. Both surface temperature trends are similar, but the temperature of the thin concrete (device B) was higher than that of the thicker concrete (device A) during the daytime. This is caused by the difference in heat capacity of the material. Therefore, the difference in *SAT* at 12:00 in Figure 4 indicates that long-wave radiation from the terrace material affected the *SAT*.

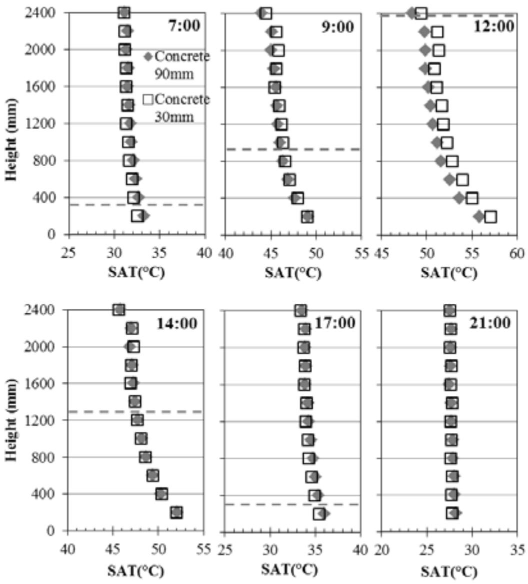

Figure 4 Vertical distribution of *SAT* for concrete.

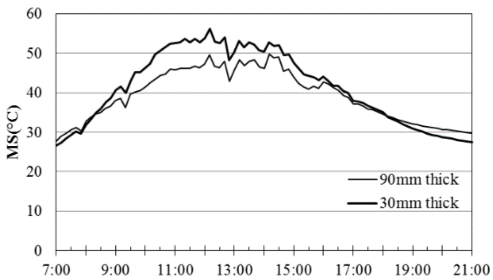

Figure 5 Surface temperature of concrete.

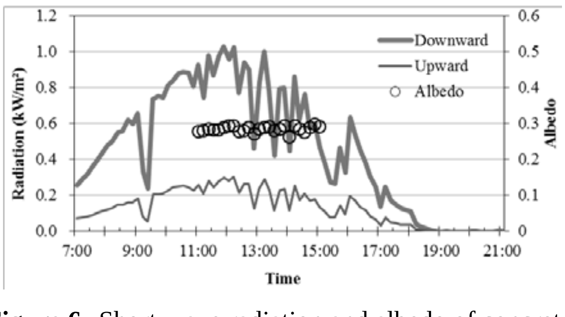

Figure 6 Short-wave radiation and albedo of concrete.

Figure 6 shows the short-wave radiation from the material in front of device B and its albedo. The albedo of the material averaged about 28% during the daytime.

3.2 Comparison of Concrete and Artificial Turf

Next, the 90-mm thick concrete tile was kept in front of device A and artificial turf was placed in front of device B.

Figure 7 shows the vertical temperature distribution of the *SAT* meters on September 5. The *SAT* distribution of device B (turf) was generally lower than that of device A (concrete). At 12:00, the difference in temperature at heights of 200 mm and 1000 mm was about 5 °C for device A (concrete) and about 3°C for device B (turf).

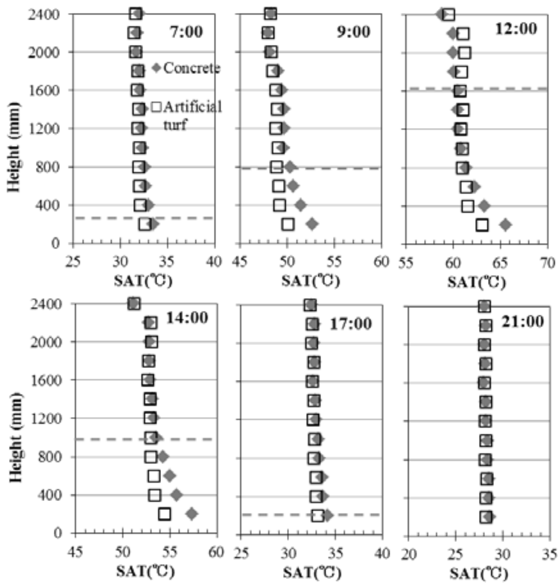

Figure 7 Vertical distribution of *SAT* for concrete and artificial turf.

At sunset, the differences in *SAT* on the upper and lower ends of the devices were small.

This indicates that both the influence of the reflection from the artificial turf and its calorific capacity are smaller than those of the concrete.

Figure 8 shows the short-wave radiation of the artificial turf and its albedo. The albedo of the artificial turf averaged about 11% during the daytime and was smaller than that of the concrete.

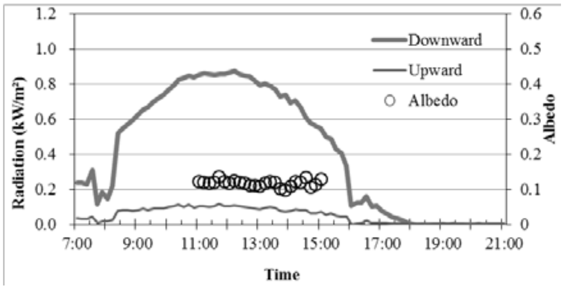

Figure 8 Short-wave radiation and albedo of artificial turf.

3.3 Comparison of Concrete and Wood Chips

Next, with the concrete tile still in front of device A, wood chips were placed in front of device B.

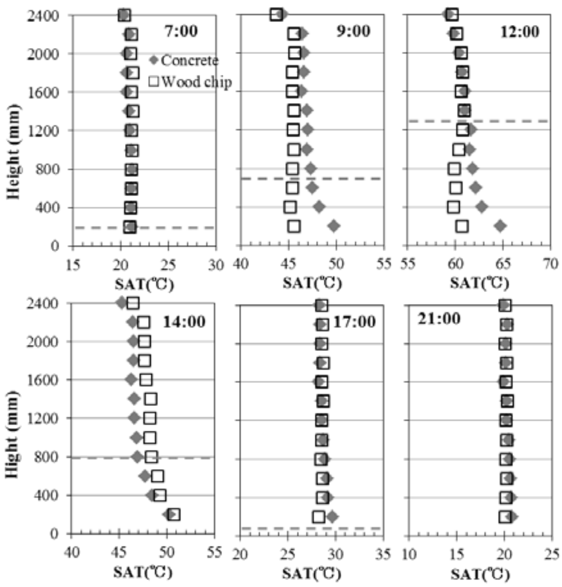

Figure 9 Vertical distribution of *SAT* for concrete and wood chips.

Figure 9 shows the vertical temperature distribution at specific times as measured by the *SAT* meter on September 21. The *SAT* distribution for device B (wood chips) was generally lower than that for device A (concrete), similar to the results with artificial turf. At 12:00, the temperature difference at heights of

200 mm and 1000 mm was about 4°C for device A (concrete) and less than 1°C for device B (wood chips). The *SAT* varied slightly from the upper to the lower end at sunset.

One factor is thought to be the influence of the varied colors and shapes of the wood chips.

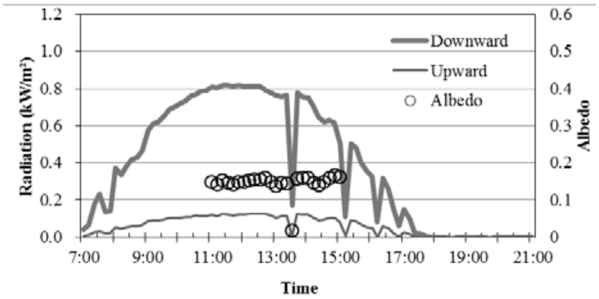

Figure 10 Short-wave radiation and albedo of wood chips.

Figure 10 shows the short-wave radiation and albedo of the wood chips. The albedo averaged about 15% during the daytime, while the solar reflectance of the wood chips, measured by an infrared spectrophotometer, ranged from 28.6% to 46.4%.

3.4 Influence of Wind

In order to confirm whether the wind affected the *SAT* during the experiment, Figure 11 shows the relationship between *SAT* (an example at a height of 200 mm) and global solar radiation. The *SAT* had a strong correlation with global

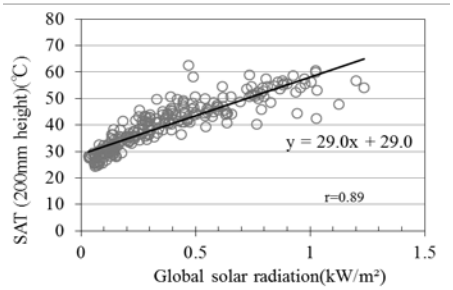

Figure 11 Relationship between global solar radiation and *SAT* at a height of 200 mm.

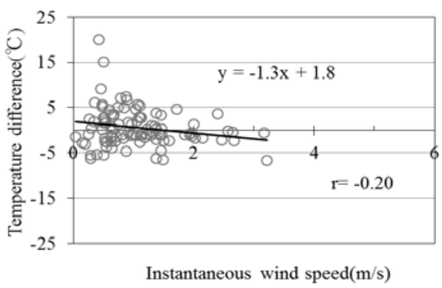

Figure 12 Relationship of instantaneous wind speed and the difference between measured and regressed temperatures.

solar radiation: the correlation coefficient was 0.89. In order to assume that there is a possibility of a temperature drop due to wind, the instantaneous value of the wind speed and the temperature differences between the regression line and *SAT* in Figure 11 were compared (Figure 12).

The temperature does show a slight downward trend as observed wind speed increased, but the correlation coefficient was only -0.20. The influence of wall and wind direction on the relationship between the convective heat transfer coefficient and wind speed near the vertical wall was relatively small [10]. Therefore, the impact of instantaneous wind speed on *SAT* is considered to be small.

4 Conclusion

In order to measure the vertical distribution of the reflected radiation to the inside of a room from terrace to building, we developed an experimental device utilizing the principle of *SAT*. The properties of 90-mm thick concrete tiles and those of other materials were compared experimentally. It was found that the reflectivity of the material had a greater effect on the vertical distribution of the radiation reflected from the surface of the terrace than the type of material. Thus this measuring device is able to grasp the effect of vertical distribution of reflected solar radiation from several terrace materials. In future work, we plan to continue to improve the performance of the experimental apparatus, as well as investigate the influence of paint color, measure other materials that have low reflectivity, and attach windows to the experimental apparatus, to determine the impact of glass.

References

[1] Akbari, H., Kurn, D., Bretz, S. & Hanford, J., *Peak Power and Cooling Energy Savings of Shade Trees*, Energy and Buildings, **25**, pp. 139-148, 1997.

[2] Tan, C.L., Wong, N.H. & Jusuf, S.K., *Effects of Vertical Greenery on Mean Radiant Temperature in The Tropical Urban Environment*, Landscape and Urban Planning, **127**, pp. 52-64, 2014.

[3] Parker, D.S. & Barkaszi, S.F.Jr., *Roof Solar Reflectance and Cooling Energy Use: Field Research Results from Florida*, Energy and Buildings, **25**, pp. 105-115, 1997.

[4] Suehrcke, H., Peterson, E.L. & Selby, N., *Effect of Roof Solar Reflectance on The Building Heat Gain In A Hot Climate*, Energy and Buildings, **40**, pp. 2224-2235, 2008.

[5] Shi, Z. & Zhang, X., *Analyzing The Effect of The Longwave Emissivity and Solar Reflectance of Building Envelopes on Energy-Saving in Buildings in Various Climates*, Solar Energy, **85**, pp. 28-37, 2011.

[6] Santamouris, M., Asimakopoulos, D.N., Asimakopoulos, V.D., Chrisomalidau, N., Klitsikas, N., Mangold, D., Michel, P. & Tsangrasoullis, A., *Energy and Climate in the Urban Built Environment*, Earthscan, pp. 110-136, 2001.
[7] de la Flor, F.J.S., Cebolla, R.O., Félix, J.L.M. & Domínguez, S.A., *Solar Radiation Calculation Methodology for Building Exterior Surfaces*, Solar Energy, **79**, pp. 513-522, 2005.
[8] O'Callaghan, P.W. & Probert, S.D., *Sol-air Temperature*, Applied Energy, **3**(4), pp. 307-311, 1977.
[9] National Astronomical Observatory of Japan, Ephemeris Computation Office Public Relations Center, http://eco.mtk.nao.ac.jp/koyomi/ (1 October 2013)
[10] Ito, N., Kimura, K. & Oka, J., *Field Experiment Study on The Convective Heat Transfer Coefficient on Exterior Surface of A Building*, ASHRAE Trans, **78**, pp. 184-191, 1972.